
MODELING OF THERMONUCLEAR FUSION FLAMES: TRANSITION TO DETONATION

A PREPRINT

Peter V. Gordon
Department of Mathematical Sciences
Kent State University
Kent, Ohio 44242, USA
gordon@math.kent.edu

Leonid Kagan*
School of Mathematical Sciences
Tel Aviv University
Tel Aviv 69978, Israel
kaganleo@tauex.tau.ac.il

Gregory Sivashinsky
School of Mathematical Sciences
Tel Aviv University
Tel Aviv 69978, Israel
grishas@tauex.tau.ac.il

April 27, 2021

ABSTRACT

The paper is concerned with identification of the key mechanisms controlling deflagration-to-detonation transition in stellar medium. The issue of thermal runaway triggered by positive feedback between the advancing flame and the flame-driven precompression is discussed in the framework of a one-dimensional flame-folding model. The paper is an extension of the authors' previous study dealing with the non-stoichiometric fusion, $fuel \rightarrow products$, kinetics (Phys.Rev.E, **103**(2021)) over physically more relevant, $fuel + fuel \rightarrow products$, kinetics. Despite this change the runaway effect endures. The transition occurs prior to merging of the flame with the flame-supported precursor shock, i.e. the pretransition flame does not reach the threshold of Chapman-Jouguet deflagration.

Keywords Supernovae explosions . White dwarfs . Thermal runaway of fast flames . Deflagration-to-detonation transition . Nucleosynthesis . Thermonuclear fusion

1 Introduction

Thermonuclear explosions of white-dwarf stars is a fundamental astrophysical issue, the first principle understanding of which is still commonly regarded as an open problem [1]. There is a general consensus that stellar explosions are manifestations of the deflagration-to-detonation transition of an outward propagating self-accelerating thermonuclear flame subjected to instability/ turbulence-induced corrugations. A similar problem arises in unconfined terrestrial flames where a positive feedback mechanism leading to the pressure runaway has been identified [2-12]. As has been recently shown [13], there is no substantial difference between terrestrial and stellar DDT events as far as physical mechanisms are concerned. Notwithstanding a considerable change in the equation of state and the reaction kinetics, the runaway effect survives. The present paper is an extension of the preceding study dealing with the non-stoichiometric fusion, $fuel \rightarrow products$, kinetics [13] over a physically more relevant, $fuel + fuel \rightarrow products$, kinetics [14,15]. In line with Ref.[13] (see also Ref.[16]), approaching the runaway point the pretransition flame may stay perfectly subsonic, thereby challenging the view that to ensure the transition the flame should cross the threshold of Chapman-Jouguet deflagration [7].

*Corresponding author

2 Formulation

Except for the altered reaction rate and some technical details (Sec.5, Appendixes A & B), the proposed new model basically follows that of Ref.[13], partially reproduced here for the convenience of the reader.

In the new formulation the planar thermonuclear fusion flame is sustained by a single-step Arrhenius-type reaction rate specified as [14,15,17],

$$W = Z\rho^2 C^2 \exp\left(-\sqrt[3]{\frac{T_a}{T}}\right), \quad (1)$$

which may imitate $^{12}\text{C}+^{12}\text{C} \rightarrow$ products, a major energy-releasing reaction in stellar flames.

Here T is the temperature; T_a , activation temperature; C , mass fraction of the reactant; ρ , gas density; Z , reaction rate prefactor.

For dense stellar matter the caloric and thermodynamic equations of state for enthalpy h and pressure p are specified as,

$$h = \frac{\gamma}{\gamma - 1} \left(\frac{p}{\rho}\right), \quad (2)$$

$$p = A\rho^\gamma + B\rho^{2-\gamma}T^2, \quad (3)$$

where γ is the adiabatic index. The caloric Eq.(2) is structurally similar to that of the ideal gas [18]. The thermodynamic Eq.(3) is a unification of classical Sommerfeld expansions pertinent to free electron gas that dominates the interior of white-dwarf stars. For the nonrelativistic and ultrarelativistic limits $\gamma = 5/3$ and $\gamma = 4/3$, respectively (see, e.g. Refs.[17, 19]).

For further discussion it is convenient to express coefficients A , B in terms of the initial pressure, densities, and temperature across the deflagration wave, assuming the latter to be isobaric. Hence,

$$p_0 = A\rho_0^\gamma + B\rho_0^{2-\gamma}T_0^2, \quad (4)$$

and

$$p_0 = A\rho_p^\gamma + B\rho_p^{2-\gamma}T_p^2, \quad (5)$$

where ρ_0, T_0, ρ_p, T_p are densities and temperatures far ahead and far behind the reaction zone in the planar isobaric flame, respectively; from here on the subscripts 0, p stand for the fresh mixture and products respectively.

Equations (4) and (5) readily imply,

$$A = \frac{p_0(\rho_p^{2-\gamma}T_p^2 - \rho_0^{2-\gamma}T_0^2)}{\rho_0^\gamma \rho_p^{2-\gamma}T_p^2 - \rho_0^{2-\gamma} \rho_p^\gamma T_0^2}, \quad (6)$$

$$B = \frac{p_0(\rho_0^\gamma - \rho_p^\gamma)}{\rho_0^\gamma \rho_p^{2-\gamma}T_p^2 - \rho_0^{2-\gamma} \rho_p^\gamma T_0^2}. \quad (7)$$

Unlike chemical ideal gas flames, Eqs. (3)-(7) allow for a significant increase of temperature ($T_p \gg T_0$) under mild thermal expansion ($\rho_p \lesssim \rho_0$), typical of thermonuclear flames [1,7,15,20,21]. Despite this distinction, the positive feedback mechanism of ideal gas flames appears to hold also in thermonuclear flames. This may be demonstrated even analytically adopting the Deshaies-Joulin approach [2] by considering the distinguished limit combing the large activation temperature with small Mach number while keeping their product finite (see Appendix A of Ref. [13] for details).

The enhancement of the flame speed in unconfined media is typically caused by instability or turbulence-induced corrugations of the reaction zone. The impact of corrugations may be accounted for even within the framework of a one-dimensional model by merely replacing the reaction rate term W by $\Sigma^2 W$ with Σ being the degree of flame front folding [2,5,6,8,9,10,12]. The Σ^2 -factor is suggested by the classical Zeldovich–Frank–Kamenetskii theory (see Ref.[13] and Sec.5 below).

For the corrugated front, $x = f(y, t)$, evolving in the channel, $0 < y < d$,

$$\Sigma = \frac{1}{d} \int_0^d \sqrt{1 + (f_y)^2} dy. \quad (8)$$

In the present formulation Σ is treated as a prescribed time-independent parameter. Note that the proposed Σ -model relates only to the deflagrative propagation and is not valid beyond the transition point. Similar to the DDT in channels (Fig.13 of Ref.[5]) the level of wrinkling (Σ) is expected to drop dramatically upon the transition.

In thermonuclear flames the energy transport prevails substantially over momentum and mass transfer thus allowing to set the Prandtl number at zero and the Lewis number at infinity [20]. In suitably chosen units the set of governing equations for one-dimensional planar geometry thus reads as follows:

Continuity,

$$\frac{\partial \hat{\rho}}{\partial \hat{t}} + \frac{\partial \hat{\rho} \hat{u}}{\partial \hat{x}} = 0, \quad (9)$$

Momentum,

$$\frac{\partial \hat{\rho} \hat{u}}{\partial \hat{t}} + \frac{\partial \hat{\rho} \hat{u}^2}{\partial \hat{x}} + \frac{1}{\gamma} \frac{\partial \hat{p}}{\partial \hat{x}} = 0, \quad (10)$$

Energy,

$$\begin{aligned} \frac{\partial \hat{\rho} \hat{E}}{\partial \hat{t}} + \frac{\partial \hat{\rho} \hat{u} \hat{E}}{\partial \hat{x}} + \left(\frac{\gamma - 1}{\gamma} \right) \frac{\partial \hat{p} \hat{u}}{\partial \hat{x}} = \\ \varepsilon \frac{\partial^2 \hat{T}}{\partial \hat{x}^2} + (1 - \sigma_p) \Sigma^2 \hat{W}, \end{aligned} \quad (11)$$

where, accounting for Eq.(2),

$$\hat{E} = \frac{1}{\gamma} \left(\frac{\hat{p}}{\hat{\rho}} \right) + \frac{1}{2} (\gamma - 1) \hat{u}^2, \quad (12)$$

Mass fraction,

$$\frac{\partial \hat{\rho} \hat{C}}{\partial \hat{t}} + \frac{\partial \hat{\rho} \hat{u} \hat{C}}{\partial \hat{x}} = -\Sigma^2 \hat{W}, \quad (13)$$

Reaction rate (see Eq.(1)),

$$\hat{W} = \hat{Z} \hat{\rho}^2 \hat{C}^2 \exp \left[N_p (1 - \hat{T}^{-\frac{1}{3}}) \right], \quad (14)$$

Thermodynamic equation of state (see Eqs.(3) – (7)),

$$\hat{p} = \hat{A} \hat{\rho}^\gamma + \hat{B} \hat{\rho}^{2-\gamma} \hat{T}^2, \quad (15)$$

where

$$\hat{A} = \frac{\sigma_p^{2-\gamma} - \theta_p^2}{\sigma_p^{2(1-\gamma)} - \theta_p^2}, \quad (16)$$

$$\hat{B} = \frac{\sigma_p^{2(1-\gamma)} (1 - \sigma_p^\gamma)}{\sigma_p^{2(1-\gamma)} - \theta_p^2}. \quad (17)$$

As may be readily checked,

$$\hat{p}(\hat{\rho} = 1, \hat{T} = 1) = \hat{p}(\hat{\rho} = \sigma_p^{-1}, \hat{T} = \theta_p) = 1. \quad (18)$$

In the above equations the basic reference scales are ρ_p , T_p , p_0 , C_0 , $h_p = \gamma p_0 / (\gamma - 1) \rho_p$, $a_p = \sqrt{\gamma p_0 / \rho_p}$, and U_p -velocity of a planar isobaric flame relative to the reaction products. Hence, $\hat{t} = t/t_p$, $\hat{x} = x/a_p t_p$, $\hat{u} = u/a_p$, $\hat{\rho} = \rho/\rho_p$, $\hat{p} = p/p_0$, $\hat{C} = C/C_0$, $\hat{E} = E/h_p$, $\hat{W} = W t_p / \rho_p C_0$, $t_p = \lambda T_p / \rho_p h_p U_p^2$, $\varepsilon = (U_p/a_p)^2$, $\sigma_p = \rho_p/\rho_0$, $N_p = \sqrt[3]{T_a/T_p}$, $\theta_p = T_0/T_p$, and λ is the thermal conductivity assumed to be constant.

In Eq.(14) \hat{Z} is the normalizing factor to ensure that under isobaric conditions ($\varepsilon \ll 1$) the scaled flame speed relative to the burned gas approaches $\Sigma \sqrt{\varepsilon}$. Evaluation of \hat{Z} is presented in the Appendix A.

Equations (9)-(17) are considered over a semi-infinite interval, $0 < \hat{x} < \infty$. The pertinent solution is required to meet the following initial and boundary conditions:

Initial conditions,

$$\begin{aligned}\hat{T}(\hat{x}, 0) &= \theta_p + (1 - \theta_p) \exp(-\hat{x}/\hat{l}), \\ \hat{C}(\hat{x}, 0) &= 1, \quad \hat{p}(\hat{x}, 0) = 1, \quad \hat{u}(\hat{x}, 0) = 0, \\ \hat{\rho}(\hat{x}, 0) &\text{ is a positive solution of Eq. (15).}\end{aligned}\tag{19}$$

Boundary conditions,

$$\begin{aligned}\partial\hat{T}(0, \hat{t})/\partial\hat{x} &= 0, \quad \hat{u}(0, \hat{t}) = 0, \quad \hat{p}(+\infty, \hat{t}) = 1, \\ \hat{T}(+\infty, \hat{t}) &= \theta_p, \quad \hat{C}(+\infty, \hat{t}) = 1, \\ \hat{\rho}(+\infty, \hat{t}) &= 1/\sigma_p, \quad \hat{u}(+\infty, \hat{t}) = 0.\end{aligned}\tag{20}$$

The parameters employed are specified as follows:

$$\begin{aligned}N_p &= 45, \quad \varepsilon = 10^{-4}, \quad \theta_p = 0.02, \quad \Sigma \geq 1, \\ \sigma_p &= 0.5, 0.85, \quad \gamma = 4/3, 5/3.\end{aligned}\tag{21}$$

The hot spot width \hat{l} of Eq.(19) is chosen to initiate the deflagrative mode. At $\Sigma > \Sigma_{DDT}$ the latter becomes unfeasible triggering transition to detonation. On the whole $50\sqrt{\varepsilon} < \hat{l} < 400\sqrt{\varepsilon}$.

In dimensional units the parameter set (21) may correspond, e.g. to $U_p = 100\text{km/s}$; $a_p = 10,000\text{km/s}$; $T_0 = 2 \cdot 10^9\text{K}$; $T_p = 10^{11}\text{K}$; $T_a = 9.1 \cdot 10^{15}$; $\rho_0 = 5 \cdot 10^9\text{g/cm}^3$; $\rho_0 = 2.5 \cdot 10^9\text{g/cm}^3, 4.25 \cdot 10^9\text{g/cm}^3$, which are quite realistic [1,7,15,20].

3 Numerical simulations

The computational method and numerical strategy employed in the present study are similar to those of Refs. [8,13]. Resolution tests are discussed in the Appendix B.

Figures 1 and 2 show $\hat{D}_f(\Sigma)$ -dependencies and spatial profiles of state variables close to the DDT point.

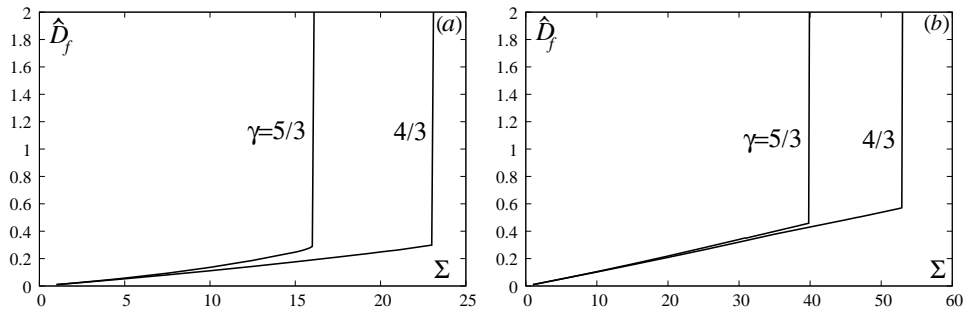


Figure 1: Scaled pre-DDT flame speed \hat{D}_f vs folding factor Σ . Two curves on each panel correspond to $\gamma = 4/3, 5/3$, $\theta_p = 0.02$, $N_p = 45$, $\sigma_p = 0.5(a)$ and $\sigma_p = 0.85(b)$

According to Fig. 1, in each case considered the flame undergoes an abrupt runaway when its speed reaches a critical level. The transition invariably occurs at $\hat{D}_f < 1$, i.e. below the threshold of the CJ-deflagration, $\hat{D}_f = 1$.

The profiles of Fig. 2 are quite in line with what is expected for a subsonic deflagration propagating from the channel's closed end [22].

4 Traveling wave solution

Behind the precursor shock the well-settled flame assumes the form of a self-similar traveling wave (Fig. 2) whose structure may be described by a single first-order ordinary differential equation (ODE) for $\hat{T}(\hat{C})$ (see Ref. [13] for

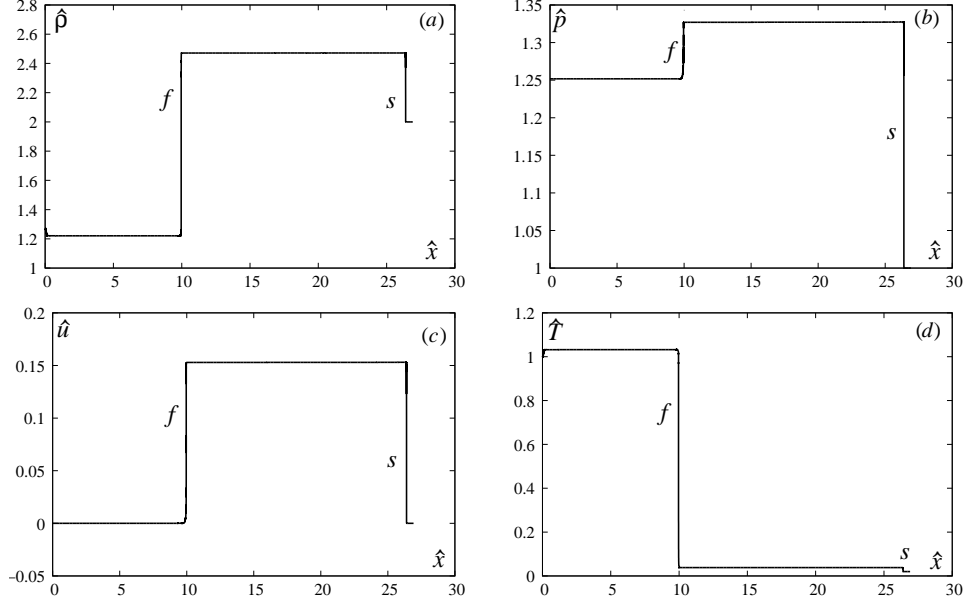


Figure 2: Spatial profiles of density (a), pressure (b), gas velocity (c), and temperature (d) adjacent to the DDT point. Labels f and s mark the flame front and the precursor shock ($\gamma = 4/3$, $\sigma_p = 0.5$, $\theta_p = 0.02$, $N_p = 45$, $\Sigma = 23$). Similar profiles for other cases of Figure 1 are not shown.

details),

$$\begin{aligned} (\hat{\rho}_1 \hat{v}_1)^2 \left[\frac{\hat{p}(\hat{T})}{\hat{\rho}(\hat{T})} + \frac{1}{2}(\gamma - 1)\hat{v}^2(\hat{T}) + (1 - \sigma_p)\hat{C} \right] + \varepsilon \Sigma^2 \hat{W} \frac{d\hat{T}}{d\hat{C}} \\ = (\hat{\rho}_1 \hat{v}_1)^2 \left[\frac{\hat{p}_1}{\hat{\rho}_1} + \frac{1}{2}(\gamma - 1)\hat{v}_1^2 + (1 - \sigma_p) \right], \end{aligned} \quad (22)$$

where $\hat{p}(\hat{T})$, $\hat{\rho}(\hat{T})$ and $\hat{v}(\hat{T}) = \hat{D}_f - \hat{u}(\hat{T})$ are defined by Eq. (15) and relations,

$$\hat{\rho}\hat{v} = \hat{\rho}_1\hat{v}_1, \quad (23)$$

$$\frac{\hat{\rho}_1^2 \hat{v}_1^2}{\hat{\rho}} + \frac{1}{\gamma} \hat{p}(\hat{\rho}, \hat{T}) = \hat{\rho}_1 \hat{v}_1^2 + \frac{1}{\gamma} \hat{p}_1. \quad (24)$$

Equation (22) is considered jointly with boundary conditions

$$\hat{T}(\hat{C} = 1) = \hat{T}_{ign}, \quad \hat{T}(\hat{C} = 0) = \hat{T}_2. \quad (25)$$

In numerical simulations the ignition temperature is set as $\hat{T}_{ign} = 1.01\hat{T}_1$.

Other relevant parameters are identical to those of Sec.2.

Parameters \hat{p}_1 , $\hat{\rho}_1$, $\hat{v}_1 = \hat{D}_f - \hat{u}_1$, \hat{T}_1 , \hat{T}_2 , \hat{D}_f may be expressed in terms of the precursor shock velocity \hat{D}_s by employing conventional Rayleigh and Rankine-Hugoniot relations across the shock and the flame front (see Ref.[13]), augmented with the equation of state (15).

The problem (22) (25) is clearly overdetermined which allows evaluation of $\Sigma(\hat{D}_f)$.

Straightforward computations show that Eq. (22) considered jointly with the first boundary condition (25) produces a family of solutions parametrized by \hat{D}_f . This family is monotone increasing with respect to Σ . This observation and standard shooting arguments allow to conclude that there exists a unique value of Σ for which the system (22)(25) admits a solution.

Figure 3 displays emerging $\Sigma(\hat{D}_f)$ -dependencies. As is readily seen the traveling wave solution ceases to exist above Σ_{max} , which invariably falls at $\hat{D}_f < 1$, i.e., below the CJ-deflagration point.

Similar to the situation in Ref.[13] only part of the $\Sigma(\hat{D}_f)$ -dependency appears to be dynamically feasible. The transition to detonation actually occurs at $\Sigma_{DDT} < \Sigma_{max}$ (Figs.1 and 4). The traveling wave solution pertaining to $\Sigma_{DDT} < \Sigma < \Sigma_{max}$ transpires to be unstable yielding an abrupt transition to CJ-detonation (cf. Ref.[13]).

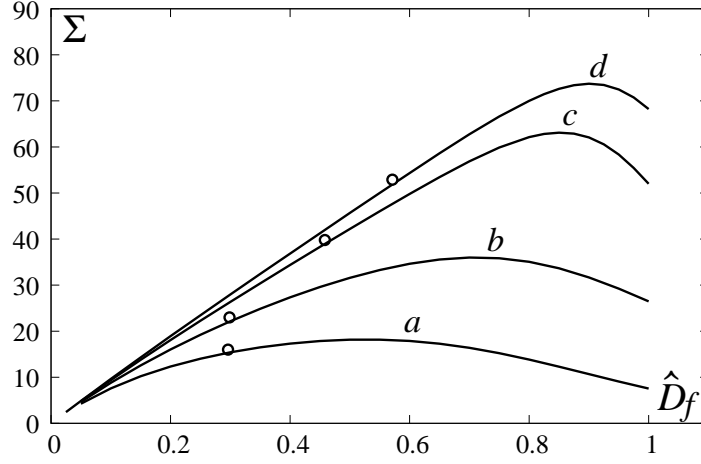


Figure 3: Folding factor Σ vs scaled flame speed \hat{D}_f , corresponding to $\gamma = 5/3$, $\sigma_p = 0.5(a)$; $\gamma = 4/3$, $\sigma_p = 0.5(b)$; $\gamma = 5/3$, $\sigma_p = 0.85(c)$; $\gamma = 4/3$, $\sigma_p = 0.85(d)$. Open circles mark the DDT points of Figure 1.

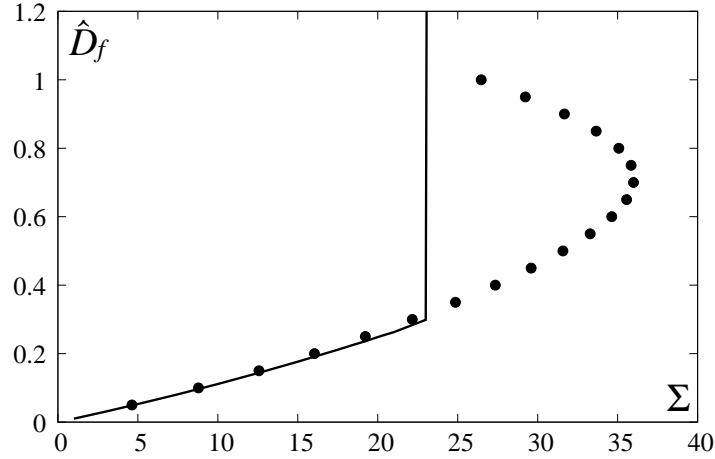


Figure 4: Illustrating the relation between the travelling wave solution (dots) and its dynamical counterpart (Figures 1 and 3) ($\gamma = 4/3$, $\sigma_p = 0.5$, $\theta_p = 0.02$, $N_p = 45$).

Figure 5 displays evolution of the reaction wave velocity \hat{D}_f emanating from the traveling wave solution corresponding to $\Sigma = 27.35$ and $\hat{D}_f = 0.4$. The incipient dynamics, upon the oscillatory deflagrative mode, abruptly converts into overdriven detonation, $\hat{D}_f > \hat{D}_{CJ}$, which eventually evolves into the Chapman-Jouguet detonation with $\hat{D}_{CJ} = 1.805$ (see Eq. (36) of Ref. [13]).

5 Concluding remarks

The Σ^2 -factor in the reaction rate term is suggested by the Zeldovich–Frank-Kamenetskii theory valid for low Mach numbers, $\hat{D}_f \ll 1$ [23]. For general Mach numbers the model is an extrapolation, expected to provide a reasonably good description of the physics involved. It is certainly satisfying that transition to detonation occurs at flame speeds \hat{D}_f , considerably below unity (see Fig. 3), which could not be foreseen in advance. Note that in the ideal gas chemical flames, e.g. at $Le = 1$, $Pr = 0.75$, $\varepsilon = 0.0025$, $\sigma_p = 0.125$, $N_p = 5$, depending on the reaction rate pressure dependency, the transition may occur either at $\hat{D}_f < 1$ or at $\hat{D}_f > 1$ [8,9].

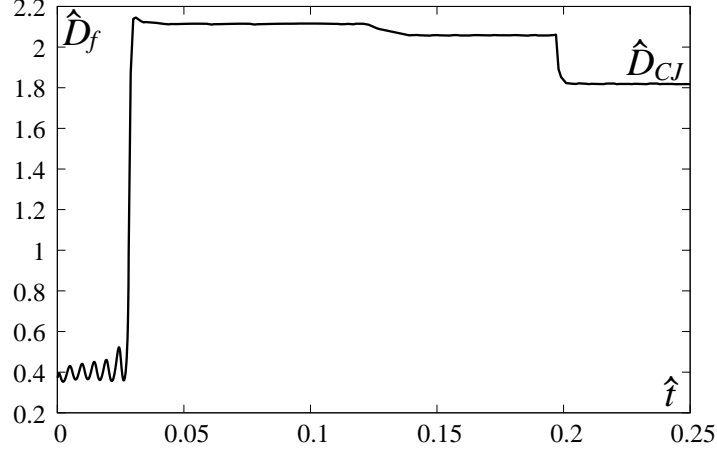


Figure 5: Time record of the reaction wave velocity \hat{D}_f . The initial conditions employed are the traveling wave profiles corresponding to $\gamma = 4/3$, $\sigma_p = 0.5$, $\theta_p = 0.02$, $N_p = 45$, $\Sigma = 27.35$.

While the one-dimensional Σ -model is helpful for exposing the precompression-induced runaway, it conceals the fine multidimensional structure of the flame-flow interaction. In the context of unconfined ideal gas chemical flames the latter issue has recently been addressed in Ref. [11] reproducing both the Darrieus-Landau (DL) wrinkling and, most importantly, DDT.

For the stellar medium however, due to the enormous disparity between the spatial scales involved, modeling and simulations of unconfined hydrodynamically unstable flames from first principles, while resolving all relevant scales, is not feasible either now or in the foreseeable future. Yet, rational development and exploration of appropriately designed reduced models (accounting for the principal physics involved) is not out of reach and is expected to be quite educational [10].

Unlike ideal gas chemical flames, in thermonuclear flames the thermal expansion of reaction products is relatively small (Sec. 2) which justifies utilization of the Boussinesq distinguished limit [24]. The Boussinesq quasi-constant-density approximation, in turn suppresses the DL-instability whose impact is generally deemed inferior to that of the Rayleigh-Taylor (RT). For a weak RT-instability the structure of the evolving flame becomes both quasi-planar and quasi-steady which allows reduction of the effective dimensionality of the problem. As a result one ends up with a weakly nonlinear equation for the flame front evolution amenable to straightforward numerical simulations [10]. The weakly nonlinear model is certainly unable to capture the full morphology of the RT-mushrooming [24]. Yet the model proves adequate enough to imitate the buoyancy-induced corrugations (Figs. 6,7), the inverse cascade, self-acceleration of the front, and occurrence of the deflagrability threshold – the precursor of DDT.

Appendix A: Evaluation of the normalizing factor \hat{Z} of Eq.(14)

To evaluate \hat{Z} we turn to the traveling wave solution of Sec.4. For the isobaric limit ($\hat{p} = 1$) the term \hat{v}^2 becomes negligibly small, $\hat{\rho}_1 = 1/\sigma_p$ and Eq. (22) simplifies to,

$$\frac{d\hat{T}}{d\hat{C}} = -\frac{(\hat{\rho}_1 \hat{v}_1)^2}{\varepsilon \Sigma^2 \hat{W}} \left[\frac{1 - \hat{\rho}(\hat{T})}{\hat{\rho}(\hat{T})} + (1 - \sigma_p) \hat{C} \right], \quad (\text{A.1})$$

where

$$\hat{A} \hat{\rho}^\gamma + \hat{B} \hat{\rho}^{2-\gamma} \hat{T}^2 = 1 \quad (\text{A.2})$$

As mentioned in Sec.2, the normalizing factor \hat{Z} is chosen to meet the condition,

$$\hat{\rho}_1 \hat{v}_1 = \Sigma \sqrt{\varepsilon} \quad (\text{A.3})$$

Equation (A.1) then assumes a form not involving parameters ε and Σ ,

$$\frac{d\hat{T}}{d\hat{C}} = -\frac{1}{\hat{Z} \hat{\rho}^2(\hat{T}) \hat{C}^2} \left[\frac{1 - \hat{\rho}(\hat{T})}{\hat{\rho}(\hat{T})} + (1 - \sigma_p) \hat{C} \right] \exp[-N_p(1 - \hat{T}^{-\frac{1}{3}})]. \quad (\text{A.4})$$

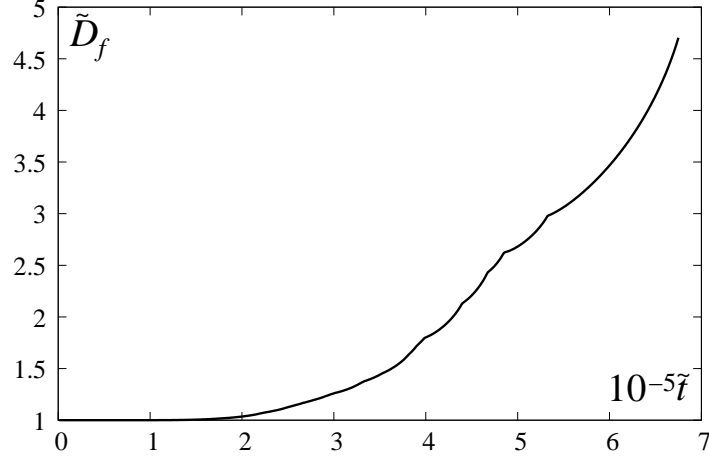


Figure 6: Scaled angle-averaged flame speed $\tilde{D}_f = \overline{R}_t$ vs. scaled time \tilde{t} at $G = 0.0002$. The reference scales employed are l_M - the Markstein length, and U_p - velocity of a planar isobaric flame relative to the reaction products, G is the buoyancy parameter [10]. At $l_M = 1\text{cm}$, $U_p = 10^6\text{cm/s}$, $\tilde{D}_{f,max}$ corresponds to $4.75 \cdot 10^6\text{cm/s}$ and \tilde{t}_{max} to 0.68s .

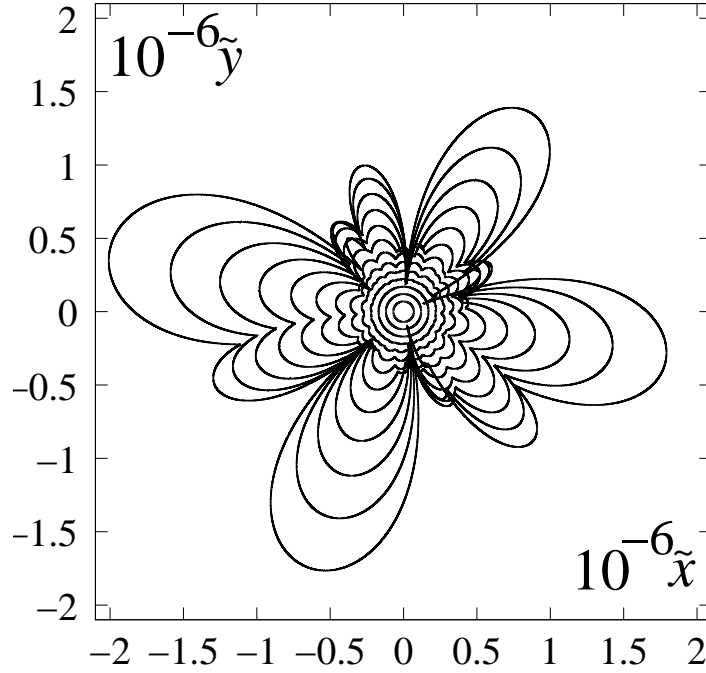


Figure 7: Flame front configurations for the weakly nonlinear model [10] prior to the DDT event at $G = 0.0002$. The reference scales employed are identical to those of Figure 6; $\tilde{R}_{max} = 2 \cdot 10^6$ corresponds to 20km .

Equation (A.4) should be considered jointly with boundary conditions,

$$\hat{T}(\hat{C} = 1) = \hat{T}_{ign}, \quad \hat{T}(\hat{C} = 0) = 1. \quad (\text{A.5})$$

The problem (A.4) (A.5), accounting for (A.2), is clearly overdetermined which allows evaluation of \hat{Z} vs N_p - dependencies calculated for $15 < N_p < 150$, $\sigma_p = 0.5, 0.85$, $\theta = 0.02$, $T_{ign} = 1.01\theta_p$, $\gamma = 4/3, 5/3$ (Fig. 8). Equation (A.4) is solved numerically with the left part of (A.5) serving as the initial condition. Parameter \hat{Z} is then determined by the bisection method.

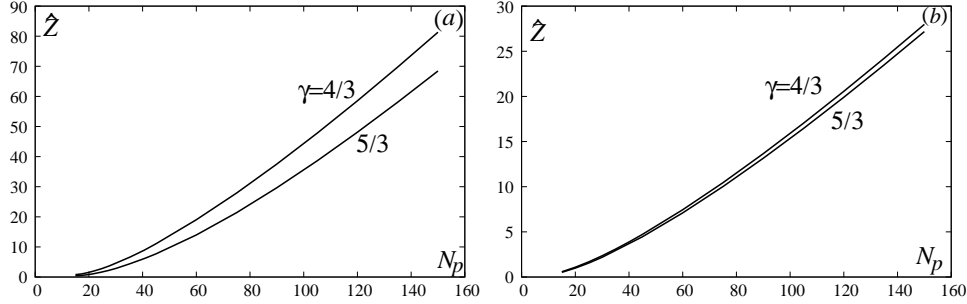


Figure 8: Normalizing factor \hat{Z} vs. N_p for $15 < N_p < 150$, $\gamma = 4/3, 5/3$, $\theta_p = 0.02$, $\sigma_p = 0.5(a)$, $\sigma_p = 0.85(b)$

Here $\hat{Z}(N_p = 45, \gamma = 4/3, \sigma_p = 0.5) = 11.181$, $\hat{Z}(N_p = 45, \gamma = 5/3, \sigma_p = 0.5) = 7.693$, $\hat{Z}(N_p = 45, \gamma = 4/3, \sigma_p = 0.85) = 4.71829$, $\hat{Z}(N_p = 45, \gamma = 5/3, \sigma_p = 0.85) = 4.45626$.

Appendix B: Localizing the runaway-point and resolution tests

Localizing the runaway-point is similar to that of Ref. [13]. The procedure is repeated for several spatial steps $\Delta \hat{x}_i = \Delta \hat{x}_{i-1}/2$. The results obtained are shown in Table 1. The last three lines are used for estimation of the convergence order (see Ref. [13]). For $\gamma = 4/3$ and $\gamma = 5/3$ the convergence orders are 1 and 0.78, predicting $\Sigma_{DDT}^0 = 55.7$ and 41.5 at $\Delta x \rightarrow 0$, respectively.

Table 1: Folding factor Σ_{DDT} at $\sigma_p = 0.85$ under different resolutions.

Δx	$\gamma = 4/3$	$\gamma = 5/3$
0.0005	40	30.8
0.00025	46.5	35.4
0.000125	51.7	38.6
0.0000625	52.5	39.8
0.000031255	52.9	40.5

For the smallest spatial steps Σ_{DDT} are close enough to Σ_{DDT}^0 . The resolutions employed are therefore quite tolerable.

Acknowledgements

The work of L.K. and G.S. was partially supported by the Israel Science Foundation (Grant 335/18). The work of P.V.G. was partially supported by the Simons Foundation (Grant 317882). The numerical simulations were performed at the Ohio Supercomputer Center (Grant PBS 0293-1) and the Computer Center of Tel Aviv University.

References

- [1] Röpke FK. 2017 Combustion in thermonuclear supernova explosions, in *Handbook of Supernovae*, edited by A. Alsabti and P. Murdin. Berlin, Heidelberg: Springer-Verlag, 1185-1209.
- [2] Deshaies B, Joulin G. 1989 Flame-speed sensitivity to temperature changes and the deflagration-to-detonation transition. *Combust. Flame* **77**, 201-212.
- [3] Gamezo VN, Poludnenko AY, Oran ES. 2011 One-dimensional evolution of fast flames, *Proceedings of the 23rd International Colloquium on the Dynamics of Explosions and Reactive Systems (ICDERS)*. Irvine, CA, paper 330.
- [4] Poludnendko AY, Gardiner TA, Oran ES. 2011 Spontaneous transition of turbulent flames to detonations in unconfined media. *Phys. Rev. Lett.* **107**, 054501.
- [5] Kagan L, Sivashinsky G. 2017 Parametric transition from deflagration to detonation. *Proc. Combust. Inst.* **36**, 2709-2715.

-
- [6] Koksharov A, Bykov V, Kagan L, Sivashinsky G. 2018 Deflagration-to-detonation transition in an unconfined space. *Combust. Flame* **195**, 163-169.
- [7] Poludnenko AY, Chambers J, Ahmed K, Gamezo V, Taylor BD. 2019 A unified mechanism for unconfined deflagration-to-detonation transition in terrestrial chemical systems and type Ia supernovae. *Science* **366**, eaa07365.
- [8] Gordon PV, Kagan L, Sivashinsky G. 2020 Parametric transition from deflagration to detonation revisited: Planar geometry. *Combust. Flame* **211**, 465-476.
- [9] Gordon PV, Kagan L, Sivashinsky G. 2020 Parametric transition from deflagration to detonation revisited: Spherical geometry. *Combust. Flame* **219**, 405-416.
- [10] Kagan L, Sivashinsky G. 2020 An elementary model for a self-accelerating outward propagating flame subject to the Rayleigh-Taylor instability: Transition to detonation. *Fluids* **5**, 196-203.
- [11] Kiverin A, Yakovenko I. 2020 Mechanism of transition to detonation in unconfined volumes. *Acta Astronautica* **176**, 647-652.
- [12] Koksharov A, Kagan L, Sivashinsky G. 2021 Deflagration-to-detonation transition in an unconfined space: Expanding hydrogen-oxygen flames. *Proc. Combust. Inst.* **38**, 3505-3511.
- [13] Gordon PV, Kagan L, Sivashinsky G. 2021 Parametric transition from deflagration to detonation in stellar medium. *Phys. Rev. E* **103**, 033106-1-9.
- [14] Fowler W, Caughlan G, Zimmerman B. 1975 Thermonuclear reaction rates, II. *Annual Review of Astronomy and Astrophysics* **13**, 69-112.
- [15] Bychkov VV, Liberman MA. 1995 Thermal instability and pulsations of the flame front in white dwarfs. *The Astrophysical Journal* **451**, 711-716.
- [16] Woosley SE, Kerstein AR, Sankaran V, Aspden AJ, Röpke FK. 2009 Type Ia supernovae: Calculation of turbulent flames using the linear eddy model. *The Astrophysical Journal* **704**, 255-273.
- [17] Clavin P, Searby G. 2016 *Combustion Waves and Fronts in Flows*. Cambridge UK, Cambridge University Press.
- [18] Landau LD, Lifshitz EM. 1980 *Statistical Physics, Part 1*, 3rd ed. Oxford, Elsevier.
- [19] Faussurier G. 2016 Equation of state of the relativistic free electron gas at arbitrary degeneracy. *Physics of Plasmas* **23**, 122704-1-14.
- [20] Timmes FX, Woosley SE. 1992 The conductive propagation of nuclear flames I. Degenerate C+O and O+Ne+Mg white dwarfs. *The Astrophysical Journal* **396**, 649-667.
- [21] Edelmann P. 2010 Modeling of thermonuclear reaction fronts in white dwarfs. *Diploma Thesis*, Technische Universität München.
- [22] Shchelkin KI, Troshin YK. 1965 *Gas Dynamics of Combustion*. Baltimore, Mono Book Corp.
- [23] Zeldovich YB, Barenblatt GI, Librovich VB, Makhviladze GM. 1985 *The Mathematical Theory of Combustion and Explosions*. New York, Plenum.
- [24] Vladimirova N, Rosner R. 2003 Model flames in Boussinesq limit: The effect of feedback. *Phys. Rev. E* **67**, 0066305.